Linewidth of high-power fiber lasers

Marc-André Lapointe [a-b], Michel Piché [b]
[a] CorActive High-Tech, 2700 Jean-Perrin, suite 121, Québec, Canada, G2C 1S9
[b] Centre d'optique, photonique et laser, Université Laval, Québec, Canada G1V 0R6

ABSTRACT

In this work, we examine how the linewidth of high-power Yb-doped fiber lasers changes as a function of laser power. Four-wave mixing between the various longitudinal modes of the laser cavity tends to broaden the laser linewidth, while Bragg reflectors have a narrow bandwidth that limits the extent of this broadening. An analytical model taking into account these effects predicts that the laser linewidth scales as the square root of laser power, in agreement with numerical simulations [1]. This model has been previously validated with a low-power Er-doped fiber laser [1] and with Raman fiber lasers [2]. In this paper, we compare the measurements taken with Yb-doped fiber lasers at power levels ranging from a few watts to hundreds of watts with the model. The broadening of high-power fiber lasers deviate from the model. Experimental data show that the linewidth broadens as a power function (between 0.5 to 1) of the laser power. A simple modification of the model is proposed which fits all the experimental data.

Keywords: laser linewidth, high-power CW fiber lasers, spectral broadening, Yb-doped fibers.

1. INTRODUCTION

High-power fiber lasers (HPFL) have generated a lot of attention over the past few years. Multi-kilowatt implementation of multimode HPFLs and kilowatt implementation of singlemode (SM) HPFLs have been achieved and commercial products are already available on the market [3]. The state-of-the-art demonstration of single mode operation of a fiber laser is currently at 6 kW [4] and prediction of SM operation at power levels exceeding 30 kW has been made [5]. The capability of fiber lasers to maintain an excellent beam quality at high power is one of their main advantages. However, there is little concern of the laser linewidth of HPFLs as they are generally used for processing of materials that have broad absorption bands.

The spectrum of fiber lasers is known to broaden with power and this phenomena is often incorrectly associated to the heating or the spectral deformation of the fiber Bragg gratings (FBG). The spectral broadening of fiber laser results from the four-wave mixing (FWM) between its $\approx 10^7$ longitudinal modes. An electronic spectral analyzer will reveal the presence of those modes by showing the Fabry-Perot axial mode spacing of the laser. V. Roy et al. [1] have validated an analytical model of the laser spectrum at low power (<100mW) with a ring Er-doped fiber laser. This model predicts that the FWM broadens the linewidth as the square root of laser power. S. Babin et al. [2] presented a detailed analytical self-consistent theory showing that FWM between longitudinal modes was the main broadening mechanism in Raman fiber lasers. Again, spectral width was determined to increase as the square root of the laser power.

The linewidth of HPFLs cannot be directly determined by the existing models because the cavity parameters are too different. The erbium ring laser used by V. Roy et al. [1] had a wide spectral filter compared to the linewidth and its non-linear phase shift ϕ_{NL} was low. On the other hand, the Raman laser used in ref. [2] had a very long cavity (300 to 1 km) where the dispersion β become non-negligible. The dispersion breaks the phase-matching condition of FWM, resulting in lower broadening. The analytical model developed in [2] is valid for cavities where the dispersion is more important than the nonlinearities. However, ϕ_{NL} of HPFLs is an order of magnitude higher than that of the Raman fiber laser and the low power fiber laser. The dispersion is also negligible because of the short cavity length (10 to 40 meters). Finally, the FBGs are very restrictive because the linewidth of the laser could become much larger than the bandwidth of the filters.

2. SPECTRAL BROADENING

2.1 Definition of spectral width

The standard deviation σ is a convenient definition for the spectral width of a non-Gaussian shaped spectrum. It is defined as the second-order moment of the spectral power distribution:

$$\sigma^2 = \int \frac{(\lambda - c)^2 P_\lambda d\lambda}{Pt}. \tag{1}$$

Eq. (1) requires the calculation of the first-order moment c. The total power Pt is the integral of the spectral power density P_λ. For a Gaussian distribution, the full width at half-height (FWHH) is 2.35σ.

2.2 The square root law

The model proposed by V. Roy et al. [1] links approximately the laser output spectrum width $\Delta\nu_{\text{out}}$ as a function of the nonlinear phase shift ϕ_{NL} and the spectral filter width $\Delta\nu_{\text{filter}}$:

$$\Delta\nu_{\text{out}} \approx \sqrt{\langle\phi_{NL}\rangle}\,\Delta\nu_{\text{filter}}. \tag{2}$$

The nonlinear phase shift $\phi_{NL}$is given as the product of the nonlinear coefficient γ, the cavity length L ant the average intra-cavity power P:

$$\phi_{NL} \approx \gamma LP. \tag{3}$$

The nonlinear coefficient γ is obtained from the nonlinear refractive index n_2, the signal wavelength λ_0 and the mode field effective area A_{eff}:

$$\gamma = \frac{2\pi n_2}{A_{eff}\lambda_0}. \tag{4}$$

S. Babin et al. [2] obtained an analytical solution to the wave-kinetic equation for the Stokes wave spectrum using a parabolic approximation of the effective FBG's reflectivity loss profile giving $\delta(\lambda) = \delta_0 + \delta_2\lambda^2$. They found that the output spectrum width $\Delta\nu_{\text{out}}$ is given by:

$$\Delta\nu_{out} = \frac{2}{\pi}\sqrt{\frac{2\phi_{NL}}{\delta_2}}. \tag{5}$$

The normal dispersion parameter β is incorporated in the nonlinear phase shift ϕ_{NL} leading to a more complex relation:

$$\phi_{NL} = \sqrt{\frac{2}{3}}\frac{\gamma LP}{1+(4\beta L/3\delta_2)^2}. \tag{6}$$

Equations (5-6) are valid for long cavities or broad FBGs if the inequality $4\beta L/\delta_2 \gg 1$ is respected. However, $4\beta L/\delta_2 \approx 0.2$ for a typical HPFL. Also, the parameter $(4\beta L/3\delta_2)^2$ is negligible for short cavities with narrow FBGs and low dispersion. In this case, the nonlinear phase shift reduce to $\phi_{NL} = \sqrt{2/3}\gamma LP$. Eq. (2) and Eq. (5) become similar at the exception of their definition of spectral width. This square root power dependence of the linewidth was named the square root law (SRL).

Generally, there are two FBGs in an HPFL, the high reflectivity FBG (HR) and the low reflectivity FBG (LR). The HR should be broader than the LR for proper operation because of the spectral broadening. In that case, the LR is the restrictive filter and its width should be used as $\Delta\nu_{\text{filter}}$ in Eq. (2). Eqs. (5-6) will provide better accuracy in the case of very similar HR and LR width but require the calculation of the loss profile. For the sake of simplicity, Eq. (2) will be used for the calculation of the spectral broadening in this work.

2.3 Nonlinear refractive index

The nonlinear refractive index n_2 of bulk silica glass yields a value $n_2 = 2.7X10^{-20}$ m^2/W at 1.06 μm [6]. However the n_2 of active silica fibers is affected by dopants such Al_20_3 and rare-earth ions. This value depends also on the technique used for the measurement and the pulse duration. For the case of FWM in CW fiber laser, n_2 could vary from 2.2 to 2.7X10^{-20} m^2/W. The value of n_2 may also decrease with the presence of pump power in ytterbium and erbium doped fiber [7]. An average value of $n_2 = 2.5$X10^{-20} m^2/W is used in this work for the calculation of the nonlinear coefficient γ.

3. RESULTS AND COMPARISON WITH THEORY: THE MODIFIED SQUARE-ROOT LAW

The spectrum of various HPFLs of different lengths and core sizes (6μm to 20μm) was measured at different value of output power ranging from a few watts to 350W. Figure 1 shows the pumping configuration of the lasers.

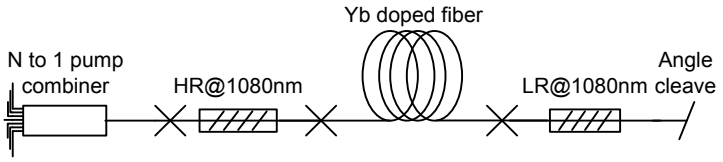

Figure 1: Schematic of the laser cavities used for the experimental measurements.

3.1 Spectral broadening of a 20/400 fiber laser

The first laser tested has an active fiber core/clad diameter of 20/400 μm. Its useful parameters are the cavity length L, the effective mode field area A_{eff}, the nonlinear coefficient γ and the spectral widths σ_{HR} and σ_{LR} of HR and LR respectively. The parameters for the 20/400 laser are given at Table 1. The FBG spectral reflectivity profiles and the output spectrum with power are shown in Figure 2. The LR has side lobes which are not present in the output spectrum.

Parameter	Value
A_{eff}	2.54X10^{-8} m^2
γ	0.57 km^{-1}W^{-1}
σ_{HR}	0.43 nm
σ_{LR}	0.25 nm
L	≈40 m

Table 1. Cavity parameters of the 20/400 fiber laser

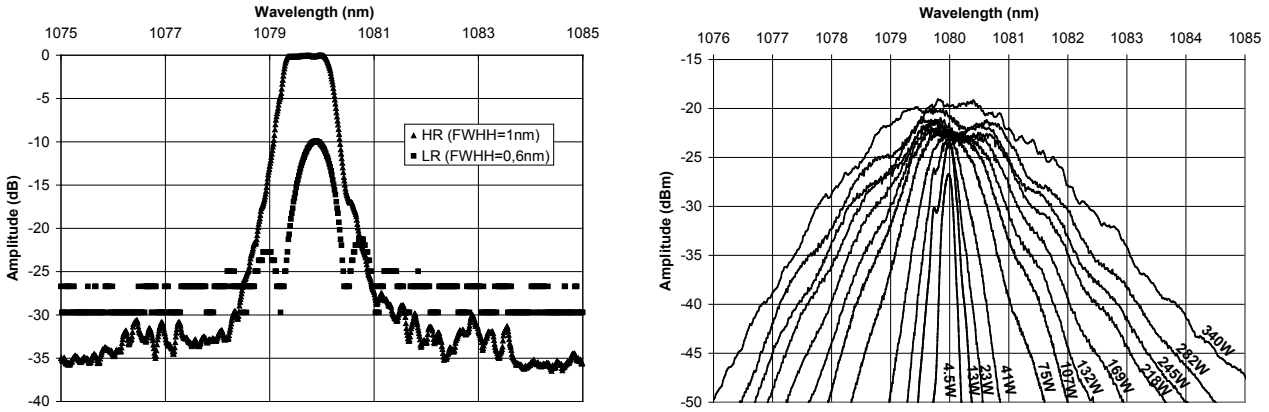

a) **b)**

Figure 2: **a)** Spectral reflectivity of the FBGs. **b)** Output spectrum of the 20/400 laser as function of power.

3.2 The modified square-root law

The experimental and theoretical values of spectral width σ_{out} as function of output power are reported in Figure 3. The theoretical spectral broadening curve of Figure 3 a) are calculated using Eq. (2) with the parameters from Table 1. The first observation from Figure 3 a) is that the spectral broadening of the lasers deviates from the SRL. The experimental data shows that $\nu_{out} \propto P^{\alpha}$ with $\alpha = 0.7$. The SRL equation can be modified to accept the fitted parameter α. This modified SRL (MSRL) defined by Eq. (7) fits the data as presented in Figure 3 b).

$$\sigma_{\text{out}} \approx \langle \phi_{NL} \rangle^{\alpha} \, \sigma_{\text{LR}} \tag{7}$$

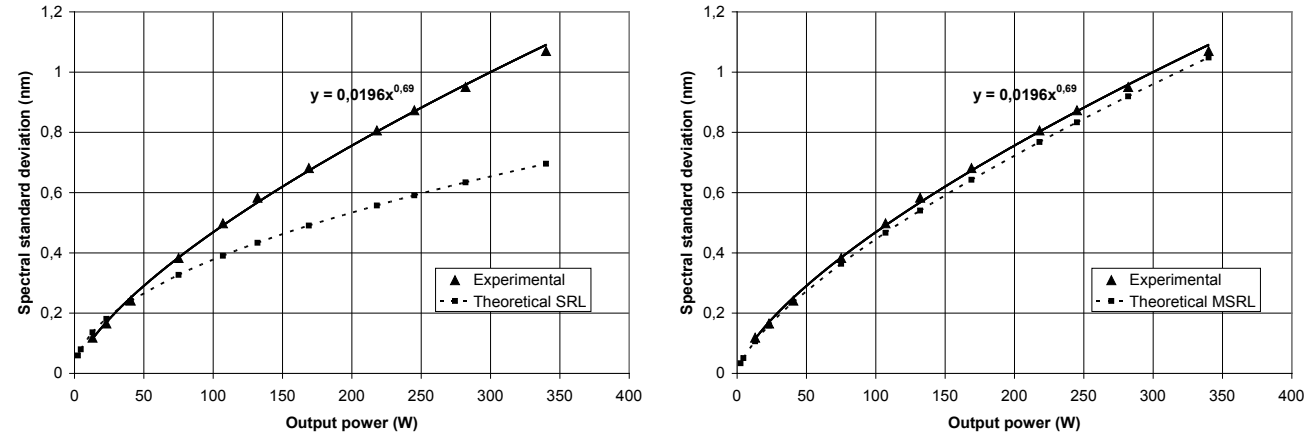

a) **b)**

Figure 3: **a)** Experimental spectral broadening with power of the 20/400 laser compared with the SRL broadening (Eq. (2)). **b)** Same as a) but using modified SRL equation (Eq. (7)) with $\alpha = 0.7$.

3.3 Spectral broadening of 12/250 fiber lasers

The MSRL is in good agreement with the experimental data from two 12/250 laser cavities (Figures 4-5) as long that the fitted parameter α is obtained from experimental data. In this particular case, the broadening is almost a linear function of the power. Also, α is relatively unchanged in Figure 5 although the cavity length L is doubled and the LR width σ_{LR} is

two times narrower. For all the tested cavities $\alpha \approx 0.5$ for the backward propagating signal. At lower power, this leads to a strange phenomenon where the spectral width of the backward propagating signal could be larger than that of the output beam as shown in Figure 5.

Parameter	Value
A_{eff}	$1.3X10^{-10}$ m^2
γ	1.1 $km^{-1}W^{-1}$
σ_{HR}	1.28 nm
σ_{LR}	0.25 nm
L	≈11 m
α	0.92

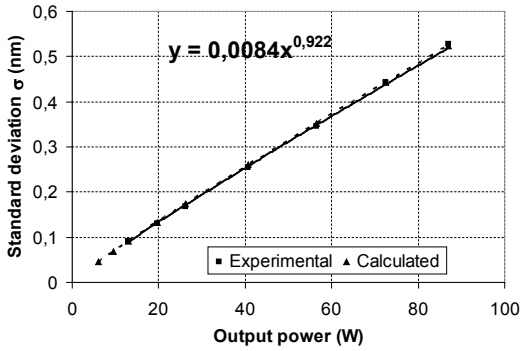

Figure 4: Output spectral broadening of a 12/250 laser with $\alpha = 0.92$.

Parameter	Value
A_{eff}	$1.1X10^{-10}$ m^2
γ	1.3 $km^{-1}W^{-1}$
σ_{HR}	1.28 nm
σ_{LR}	0.25 nm
L	≈22 m
α	0.98

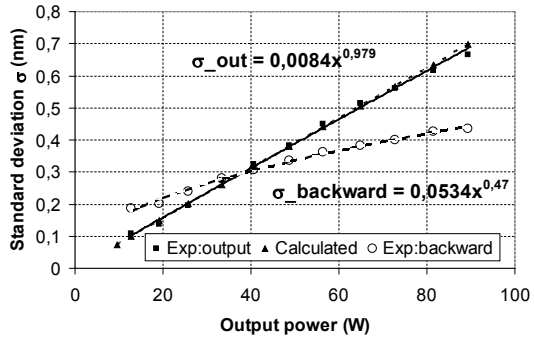

Figure 5: Output and backward spectral broadening of a 12/250 laser with $\alpha = 0.98$.

3.4 Spectral broadening of a 10/200 fiber laser

A smaller MFD induces a higher nonlinear coefficient γ. Thus, there is more broadening in a laser with 10/200 fibers as presented in Figure 6. Like for 20/400 laser, α is in the range of 0.7. At 50W of output power, the linewidth is 4 times the LR width.

Parameter	Value
A_{eff}	$5.59X10^{-11}$ m^2
γ	2.6 $km^{-1}W^{-1}$
σ_{HR}	0.42 nm
σ_{LR}	0.22 nm
L	≈33 m
α	0.72

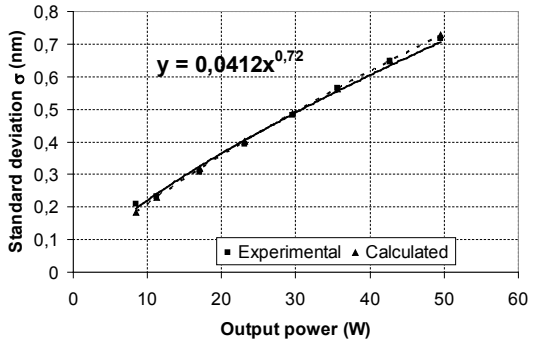

Figure 6: Output spectral broadening of a 10/200 laser with $\alpha = 0.72$.

3.5 Spectral broadening of 6/125 fiber lasers

Again, α is in the range of 0.7 for the cases of Figure 7 and Figure 8. For Figure 8, 33 meters of passive fiber were inserted into the cavity to observe the increased broadening. The average nonlinear coefficient is used for the calculation of Eq. (6).

Parameter	Value
A_{eff}	$3.74X10^{-11}$ m^2
γ	3.9 $km^{-1}W^{-1}$
σ_{HR}	1.28 nm
σ_{LR}	0.25 nm
L	≈33m
α	0.76

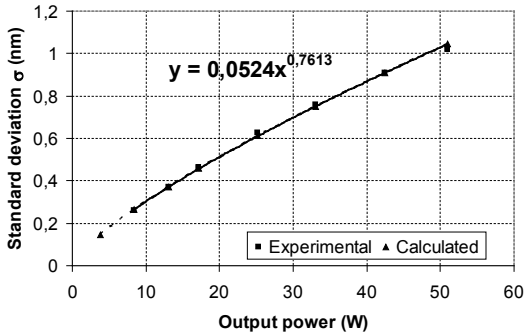

Figure 7: Output spectral broadening of a 6/125 with $\alpha = 0.76$.

Parameter	Average Value	Yb fiber	Passive
A_{eff}	$4.5X10^{-11}$ m^2	$3.74X10^{-11}$ m^2	$6.0X10^{-11}$ m^2
γ	3.2 $km^{-1}W^{-1}$	3.9 $km^{-1}W^{-1}$	2.4 $km^{-1}W^{-1}$
σ_{HR}	1.28 nm		
σ_{LR}	0.25 nm		
L	≈63m	33	30
α	0.72		

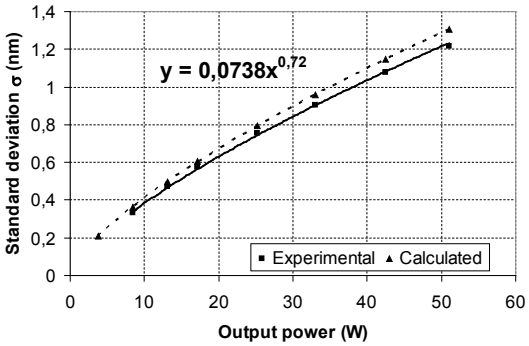

Figure 8: Output spectral broadening of a 6/125 with $\alpha = 0.72$. 33 meters of passive fiber were inserted into the cavity.

Finally, a flat cleave was done to create a Fresnel reflection and replace the LR FBG. This configuration, where $\sigma_{HR} < \sigma_{LR}$, generates a particular backward spectrum that is shown in Figure 9 . The spectral reflectivity profile of the HR is visible in the backward spectrum because the signal was leaking through the HR. At full power, the total power returning to the pump (>4W) was 50 times higher than with the standard configuration where $\sigma_{HR} > \sigma_{LR}$. Also, the linewidth did not coincide with the center of the HR bandwidth, causing a decrease of the effective HR width to approximately $\sigma_{HR} \approx 0.5nm$. The cavity parameter and the linewidth broadening curve for this configuration are shown in Figure 10. There is more broadening in this case because $\Delta\nu_{\text{filter}}$ is doubled. However, the power dependence α is now ≈ 0.5.

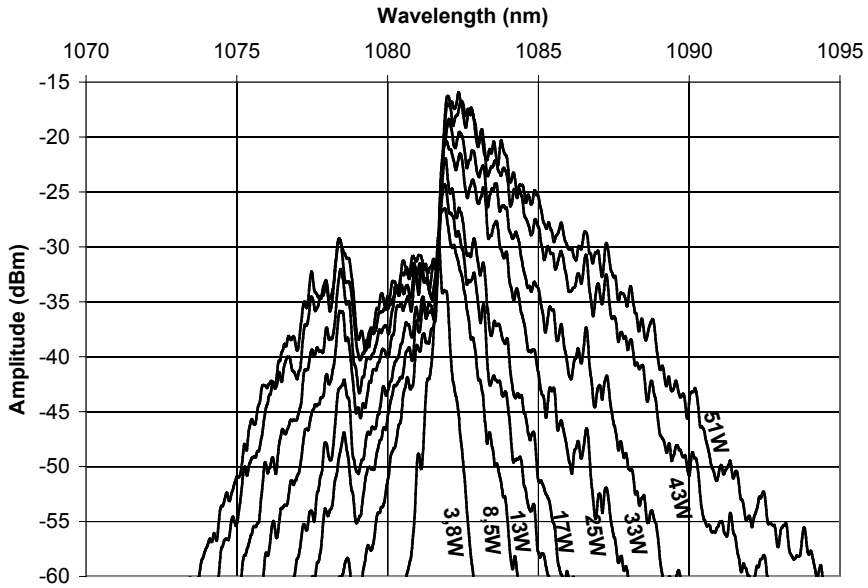

Figure 9: Backward spectrum at the pump combiner as function of output power of a 6/125 laser in which a flat cleave is replacing the LR FBG.

Parameter	Value
A_{eff}	$3.74X10^{-11}$ m^2
γ	3.9 $km^{-1}W^{-1}$
σ_{HR}	0.5nm
σ_{LR}	Fresnel reflection
L	≈33m
α	0.54

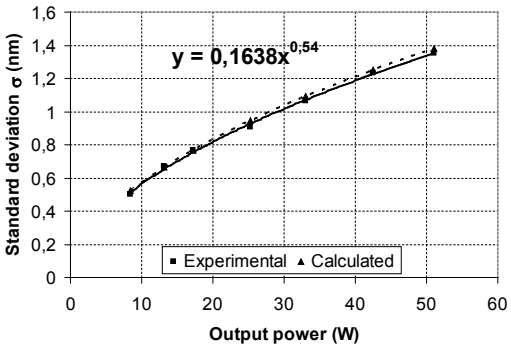

Figure 10: Output spectral broadening of a 6/125 laser with $\alpha = 0.54$. A flat cleave is used to replace the LR FBG.

4. CONCLUSION

Experimental results on the spectral broadening of high-power fiber laser (HPFLs) were compared with an existing theory of four-wave mixing (FWM). It was shown that the FWM is the dominant broadening mechanism in HPFLs. But experimental data deviate from the theoretical square-root law relationship that was previously validated for a low power erbium ring fiber laser [4] and long Raman fiber lasers [5]. FWM increases the linewidth of HPFLs as a function of power with an exponent α between 0.5 and 1. The theoretical model was modified to include the fitted value of exponent α. This modified model is in good agreement with all experimental data. A large spectral broadening affects slope efficiency and causes leakage of power through the high-reflectivity mirror.

ACKNOWLEDGEMENTS

This work has benefited from the financial support from CorActive High Tech and Laval University. Marc-André Lapointe was supported by an FQRNT-NSERC scholarship awarded through the BMP "Photonics" program managed in collaboration with the Canadian Institute for Photonic Innovations (CIPI).

REFERENCES

[1] Roy, V., Piche M., Babin, F., Schinn, G., "Nonlinear wave mixing in a multilongitudinal mode erbium-doped fiber laser," Optics Express, vol. 13, 6791-6797 (2005).

[2] Babin, S., Churkin, D., Ismagulov,A., Kablukov, S., Podivilov, E., "Four-wave-mixing-induced turbulent spectral broadening in a long Raman fiber laser," Journal of the Optical Society of America B (Optical Physics), vol. 24, 1729-38 (2007).

[3] IPG Photonics, http://www.ipgphotonics.com.

[4] Gapontsev, D., "6kW CW single mode ytterbium fiber laser in all-fiber format", 21st Annual Solid State and Diode Laser Technology Review, 258 (2008).

[5] Dawson, J.W. , Messerly, M.J. , Beach, R.J., Shverdin, M.Y. , Stappaerts, E.A. , Sridharan, A.K., Pax, P.H., Heebner, J.E. , Siders, C.W. , Barty, C.P.J. , "`Analysis of the scalability of diffraction-limited fiber lasers and amplifiers to high average power", Optics Express, vol. 16 no. 17, 13240-13266 (2008).

[6] Agrawal, G.P, [Nonlinear Fiber Optics], Academic press, San Diego, 447-451 (2001).

[7] Garcia, H., Johnson, A.M., Oguama, F.A., Trivedi, S., "Pump-induced nonlinear refractive-index change in erbium- and ytterbium-doped fibers: theory and experiment," Optics Letters. vol. 30, 1261-1263 (2005)